

Electric feedback cooling of single charged nanoparticles in an optical trap

M. Iwasaki,¹ T. Yotsuya,¹ T. Naruki,¹ Y. Matsuda,¹ M. Yoneda,¹ and K. Aikawa¹

¹*Department of Physics, Tokyo Institute of Technology, Ookayama 2-12-1, Meguro-ku, 152-8550 Tokyo*

(Dated: December 15, 2024)

We demonstrate feedback cooling of the center-of-mass motion of single charged nanoparticles to millikelvin temperatures in three dimensions via applying oscillating electric fields synchronized to their optically observed motion. We develop a model for the electric feedback process and show that the observed motional temperature at weak feedback agrees quantitatively with our model. The agreement between our model and experiments is confirmed by independent measurements of the charge numbers based on a shift in the oscillation frequency induced by a constant electric field. The demonstrated cooling efficiency prevails over that of the conventional cooling method with the parametric modulation of the trapping potential. Our results form the basis of manipulating cold charged nanoparticles and paves the way to quantum mechanical studies with trapped nanoparticles near their ground state.

Manipulating the motion of objects near their quantum ground state has been a crucial subject in diverse fields from quantum simulations [1–3] and quantum information processing [4] to precision measurements [5, 6]. Cooling atomic ions and ensembles of neutral atoms to their motional ground state has been successful [2, 7]. Specific vibrational modes of nano- and micromechanical oscillators have been brought to their quantum ground state [8, 9]. However, cooling the motion of particles including more than a few atoms to their motional ground state has been an elusive goal. The main difficulty lies in the absence of an efficient mechanism for cooling.

Cold nanoparticles are expected to possess various applications such as testing quantum mechanics for macroscopic objects [10, 11], ultrasensitive force and mass sensing [12–18], and the laboratory test of the collisional dynamics of interstellar materials [19]. Up to now, cooling the motion of nanoparticles to millikelvin temperatures has been demonstrated via all-optical approaches, where trapping, observing, and cooling them are all based on light scattering [20–25]. The lowest temperature achieved with all-optical approaches is finally limited by random photon recoils [26]. To overcome the limitation from photon recoils, an all-electrical approach for highly charged particles has been proposed [27].

Here, we show that the motional temperature of single charged nanoparticles in an optical trap is efficiently lowered via the optical measurement of the nanoparticle's position and the application of oscillating electric fields synchronized to their motion. We develop a theoretical model that describes the electric feedback process. The observed motional temperatures with the electric feedback T_{eff} agree quantitatively with our model only when the mass of the nanoparticle is properly estimated with the time scale of the rethermalization of the motion after it is cooled. The agreement between our model and experimental results is confirmed by independent measurements of the charge number based on the electric-field-induced shift in the oscillation frequency.

Compared to the conventional all-optical cooling method, parametric feedback cooling (PFC) [21, 24], our method, electric feedback cooling (EFC), has two important advantages. First, because the magnitude of the electric force is independent from T_{eff} , EFC has a high cooling rate, while in PFC

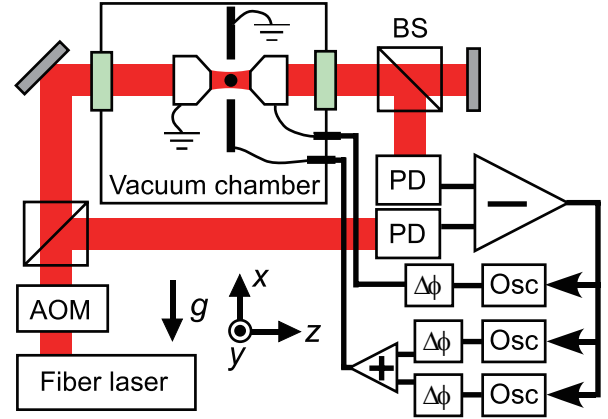


FIG. 1. (color online). Schematic representation of our experimental setup. The center-of-mass motion of an optically trapped charged nanoparticle is observed via a balanced photodetector. Three oscillators locked to the photodetector signal provide time-varying electric fields with optimum phases and frequencies, which cool the motion of the nanoparticle in three dimensions. The electrodes perpendicular to the trapping beam is tilted by 45° with respect to the x direction such that they provide electric fields in both x and y directions.

the cooling rate is proportional to T_{eff} [21]. Second, in EFC, the feedback signal is purely electrical, and thus does not perturb the optical position measurement, whereas, in PFC, the modulation on the trapping potential for cooling can affect the position measurement. In the present work, we demonstrate T_{eff} below 10 mK at 4×10^{-3} Pa, which is about one order of magnitude lower than the values obtained with PFC at this pressure, manifesting the efficiency of our approach.

In our experiments, we trap silica nanoparticles with radii of about 100 nm in a one-dimensional optical lattice formed with a fiber laser at $\lambda = 1550$ nm (Fig. 1) [28, 29]. We observe the three-dimensional motion of nanoparticles with a photodetector measuring the spatio-temporal variation of the infrared light scattered by them [24]. The area of the power spectral density (PSD) calculated from the photodetector signal is proportional to T_{eff} [21, 24]. When the chamber is evacuated, trapped nanoparticles are positively ionized [30]. Two objective lenses and two wires work as electrodes for applying

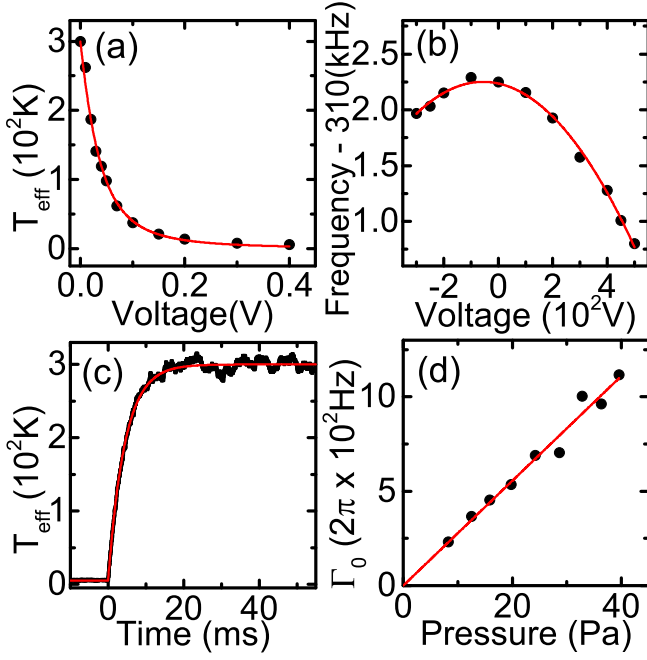


FIG. 2. (color online). A series of measurements for finding the properties of trapped nanoparticles. All the data are taken for a specific nanoparticle. (a) T_{eff} in the z direction as a function of the applied voltage amplitude at 13 Pa. The phases of feedback signals are adjusted to give minimum temperatures. The solid line is a fit with eq.(3). (b) The oscillation frequency in the z direction as a function of the applied dc voltage. A fit with eq.(4) is shown by a solid line. The maximum in the oscillation frequency lies at a finite electric field, where the residual gradient, mainly due to the radiation pressure, is compensated by the electric force. The curvature of the frequency variation reflects the value of n . (c) Time evolution of T_{eff} in the z direction averaged over 256 traces. EFC is turned off at 0ms. The solid line is an exponential fit. The exponential time constant is the inverse of Γ_0 . (d) Measured Γ_0 with respect to the pressure. The solid line is a linear fit without intercept.

three-dimensional electric fields around the trapping region.

The motion of a trapped charged nanoparticle is continuously attenuated if an applied electric field switches its sign in phase with the nanoparticle's motion and provides an electric force opposite to its velocity. Understanding on such a process is achieved by considering the following model. We describe the motion of nanoparticles in a specific direction in the presence of an electric field by the one-dimensional equation of motion:

$$\ddot{q} + (\Gamma_0 + \Gamma_c)\dot{q} + \Omega_0^2 q = \frac{F_{\text{fl}}}{m} \quad (1)$$

where q , Γ_0 , Γ_c , Ω_0 , m , and F_{fl} denote the position of nanoparticles, the damping rate due to collisions with background gases, the damping rate due to an electric force, the oscillation frequency of the motion of nanoparticles given by the laser confinement, the mass of trapped nanoparticles, and a stochastic force from background gases, respectively. To a good approximation, Γ_0 is proportional to the background pressure at our working pressure range and is given by [21, 24]

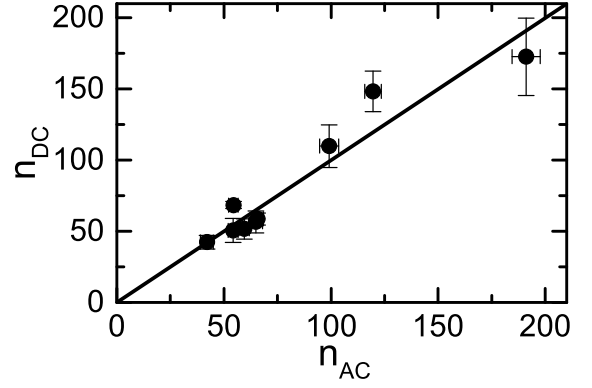


FIG. 3. Comparison of measured charge numbers, n_{AC} and n_{DC} , for different nanoparticles trapped during multiple experimental runs. The solid line shows $n_{\text{AC}} = n_{\text{DC}}$ and is not a fit. The agreement between n_{AC} and n_{DC} is a direct proof that the properties of trapped nanoparticles are correctly measured.

$$\Gamma_0 = 0.619 \frac{9\pi\zeta d_m^2 P}{\sqrt{2}\rho k_B T_0 R} \quad (2)$$

where ζ , d_m , P , ρ , k_B , T_0 , and R are the viscosity of air, the diameter of an air molecule, the pressure, the density of the particle, the Boltzmann constant, the temperature of background gases around the trapped nanoparticle, and the radius of the particle, respectively. Considering that the electric force is given as an amplitude of neV/d_{eff} multiplied by a sinusoidal time variation of $\dot{q}/(q_0\Omega_0)$, where n is the charge number, e is the elementary charge, V is the applied voltage amplitude, d_{eff} is the effective distance between electrodes, and q_0 is the amplitude of the motion at equilibrium, we find $\Gamma_c = neV/(m\Omega_0 q_0 d_{\text{eff}})$. The effective motional temperature at equilibrium T_{eff} is then given by [31]

$$\frac{T_{\text{eff}}}{T_0} = \left(\sqrt{1 + A^2} - A \right)^2, \quad A = \frac{neV}{2\Gamma_0 d_{\text{eff}} \sqrt{mk_B T_0}} \quad (3)$$

Our model suggests that T_{eff} smoothly decreases from T_0 with increasing the value of A . We experimentally confirm such a behavior by measuring T_{eff} for various voltage amplitudes at a fixed pressure [Fig. 2(a)]. We realize cooling trapped nanoparticles in three dimensions by applying electric fields provided by three oscillators independently locked to the photodetector signal (Fig. 1). The effective distance between two electrodes for the z direction is numerically determined to be $d_{\text{eff}}^z = 5.0(1)$ mm. The observed profile is in good agreement with the fitted curve based on our model, showing that our model provides a good understanding on the cooling process.

In what follows, we show that the observed cooling behavior [Fig. 2(a)] agrees quantitatively with our model and is a good measure for testing if we have good knowledge on the properties of trapped nanoparticles. For each experimental run, we need to measure the mass and the charge number of

the trapped nanoparticle. The mass can be derived from R obtained with eq.(2) if Γ_0 is correctly measured. While the fit on the temperature decrease in Fig. 2(a) allows us to derive the value of n , which we denote as n_{AC} , the value obtained in this way may be wrong if Γ_0 is not properly measured. For the purpose of checking consistency between these parameters, in the present study, we introduce a new method for determining n independently from the measurement of Fig. 2(a).

We apply a dc electric field and observe an induced shift in the oscillation frequency in the z direction. The presence of a gradient shifts the position of the potential minimum, at which the oscillation frequency is lowered due to the anharmonicity of the potential. Because the optical lattice has a well-defined sinusoidal structure with a spacing of $\lambda/2$, we are able to measure the applied gradient precisely. The oscillation frequency in the z direction in the presence of a dc voltage V is given by [31]

$$\Omega_z = \Omega_{z0} \left[1 - \left\{ \frac{4\pi(neV/d_{\text{eff}} + F_0)}{m\Omega_{z0}^2\lambda} \right\}^2 \right]^{1/4} \quad (4)$$

where Ω_{z0} is the oscillation frequency in the absence of gradients and F_0 is the offset gradient mainly due to the radiation pressure exerted by the trapping laser [32]. When we measure the oscillation frequency as a function of the magnitude of the applied voltage, we find that the observed frequency variation is in good agreement with the above expression [Fig. 2(b)]. From the curvature of this plot, we obtain the value of n , which we denote as n_{DC} . Considering the dependence of $m \propto \Gamma_0^{-3}$, we find that the two methods for determining n have different dependences on Γ_0 : $n_{AC} \propto \Gamma_0^{-1/2}$ and $n_{DC} \propto \Gamma_0^{-3}$. This fact indicates that unless the value of Γ_0 is properly measured we encounter an unrealistic result of $n_{AC} \neq n_{DC}$. In fact, with the conventional method for determining Γ_0 , i.e., extracting the spectral width from the PSD [21, 24], we found large discrepancies between n_{AC} and n_{DC} by up to a factor of 10. We infer that the discrepancy originates from various technical issues such as fluctuations of the optical system and errors in fitting the PSD.

We find that the reliable way to determine Γ_0 is to observe the time evolution of T_{eff} [33]. We first prepare trapped nanoparticles cooled via EFC to arbitrary temperatures. After EFC is turned off, we observe an exponential growth of T_{eff} [Fig. 2(c)]. The time constant of the growth directly reveals Γ_0 . We confirm that at our working pressure range the measured values of Γ_0 are proportional to the pressure as expected from eq.(2) [Fig. 2(d)]. Using the value of Γ_0 obtained in this way, we arrive at a reliable value of n with n_{AC} and n_{DC} agreeing within 30%. For the specific case of the presented data in Fig. 2, the mass and the charge number are determined to be $m = 1.6(1) \times 10^{-17}$ kg and $n_{DC} = 59(4)$, where the errors are dominated by the error in determining Γ_0 . Within a single experimental run, n stays constant, while it varies between 10 and 300 among many experimental runs. The comparison between n_{AC} and n_{DC} for multiple experimental runs is shown in

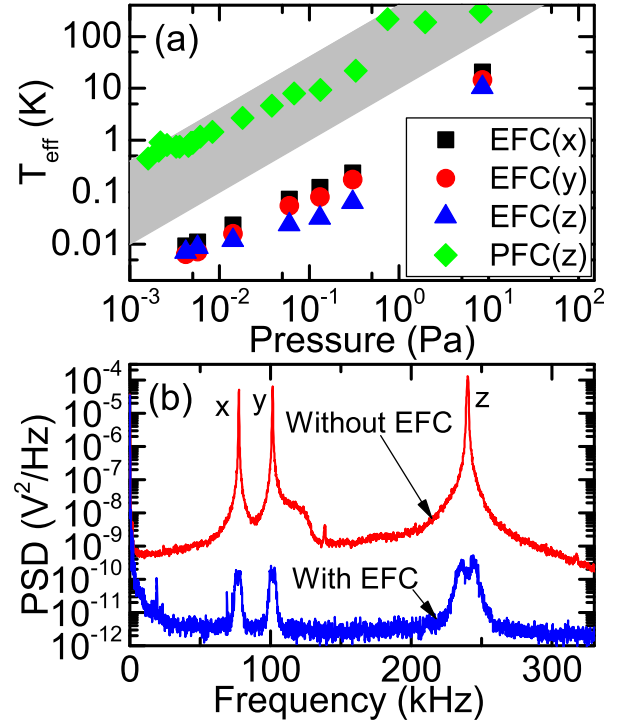


FIG. 4. (color online). (a) T_{eff} obtained with EFC as a function of the pressure. The phase and the amplitude of feedback signals are adjusted to give minimum temperatures in each direction. The shaded area shows typical cooling results with PFC. Our results on PFC of a nanoparticle, a different one from the one used for EFC, in the direction of the optical lattice is also presented. (b) The PSDs without EFC at 16 Pa and with EFC at 4×10^{-3} Pa.

Fig. 3. In our system, we have not succeeded in observing the variation of n by a single e , which was used to determine n in previous work [30]. We infer that this is because the charge variation in our system is much larger than in the previous work.

In the above analysis, we have assumed $T_0 = 300$ K as in previous works on PFC [21, 24]. Although this assumption is reasonable in the pressure range of Fig. 2, recent work has shown that T_0 can be higher than room temperature at high vacuum due to heating associated with laser absorption [33, 34]. Having a look at the representations in eqs.(2-4), we realize that n_{AC} and n_{DC} have different dependences on T_0 : $n_{AC} \propto T_0^{-1}$ and $n_{DC} \propto T_0^{-3}$. For quantitatively observing the influence of increased T_0 , we need an independent measurement on the absolute motional temperature, which can be realized in our setup in the following manner. First, the conversion factor between the voltage of the photodetector and the nanoparticle's displacement should be determined by comparing the amount of the free fall of sufficiently cooled nanoparticles and the corresponding voltage signal. Free-fall measurements on cold nanoparticles has been recently implemented for the purpose of force sensing [18] and is technically feasible. Using this conversion factor, we can derive the temperature value as $T_{\text{eff}} = m\Omega_0^2 q_0^2 / k_B$. Calibration of the PSD in

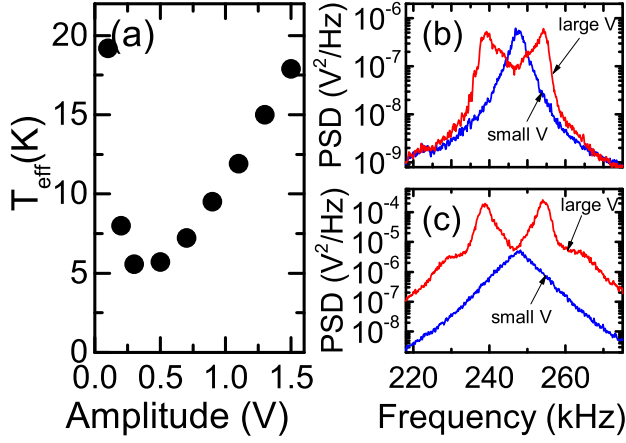


FIG. 5. (color online). (a) T_{eff} in the z direction as a function of the applied voltage amplitude. (b) PSDs of the motion of trapped nanoparticles in the z direction at small (0.2 V) and large (1.3 V) voltage amplitudes. (c) PSDs of the feedback signals for (b). At large voltage amplitudes, the feedback loop starts to oscillate at around the frequency of the bandwidth, resulting in increased T_{eff} .

other methods has been reported [18, 35].

Our model suggests that decreasing Γ_0 , which is achieved by decreasing the pressure, reduces T_{eff} . In fact, we observe a dramatic decrease in T_{eff} as the pressure is lowered [Fig. 4(a)]. For comparison, we also show typical results obtained in previous work on PFC [21, 24] and our results obtained with PFC. We find that within our working pressure range of $4 \times 10^{-3} \sim 100$ Pa, the temperature obtained with EFC is lower than that with PFC by one to two orders of magnitude. The lowest observed temperature in the present work is about 10 mK at 4×10^{-3} Pa for all directions. The PSDs with and without the electric feedback are shown in Fig. 4(b).

Finally, we address an important aspect regarding the limit of cooling. According to our model, T_{eff} should be infinitely decreased at infinitely large voltage amplitudes, which is opposed to our observation that the lowest achievable temperature is finite and varies at each pressure. We find that at each pressure there exists an optimum voltage amplitude, above which T_{eff} increases (Fig. 5). Such a limitation originates from the finite feedback bandwidth. When the voltage amplitude is increased, we observe that the feedback loops starts to oscillate at around 10 kHz, which approximately coincides with the bandwidth of the phase lock loop (PLL) for locking the oscillators to the photodetector signals. Outside the bandwidth, the phase of the feedback signal is delayed by more than 180° , amplifying the nanoparticle's motion instead of attenuating it. Though increasing the PLL bandwidth is possible, this makes the PLL at low frequency inferior and also results in the increased T_{eff} . Thus, in the current setup, we have a limitation on the lowest achieved temperature originating from the PLL bandwidth. Note that this issue is not a fundamental problem in our cooling approach and can be overcome with a technical upgrade, e.g., to use filtered photodetector signals directly for

feedback.

In conclusion, we demonstrate an efficient approach for cooling the center-of-mass motion of single optically trapped nanoparticles via the combination of the optical observation of the particle position and the application of electric fields synchronized to their motion. We develop models for describing the response of charged particles to ac and dc electric fields and confirm that observed behaviors are in good agreement with our models. The demonstrated temperatures of below 10 mK at 4×10^{-3} Pa are about one order of magnitude lower than that with the conventional method based on the parametric modulation of the optical potential. The advantages of our approaches lie in the strong cooling force independent from T_{eff} and the clean observation signals unaffected by feedback signals. We envision that even lower temperature can be achieved at lower pressures. At low pressures, the motion of laser-trapped nanoparticles is heated by random photon recoils [26]. The high cooling rate of our approach is expected to be beneficial for reaching an unprecedented temperature regime near the quantum ground state, paving the way to explore quantum physics for macroscopic objects. Our cooling strategy is also applicable to particles trapped in an ion trap, where they can be observed with a weak probe laser that has a minimum heating effect. Furthermore, our approach allows us to prepare cold nanoparticles for various measurements such as calibration of the PSD and force sensing even at medium vacuum.

We thank M. Ueda and M. Kozuma for fruitful discussions. This work is supported by the Murata Science Foundation, the Mitsubishi Foundation, the Challenging Research Award and the 'Planting Seeds for Research' program from Tokyo Institute of Technology, Research Foundation for Opto-Science and Technology, JSPS KAKENHI (Grants No. JP16K13857 and JP16H06016), and JST PRESTO (Grant No. JPMJPR1661).

SUPPLEMENTARY INFORMATION

Derivation of the effective temperature under an electric feedback force

The PSD of single particles following the equation of motion [eq.(1)] is given by

$$S(\omega) = \frac{k_B T_0 \Gamma_0}{\pi m} \frac{1}{(\Omega_0^2 - \omega^2)^2 + \Gamma_{\text{tot}}^2 \omega^2} \quad (5)$$

with $\Gamma_{\text{tot}} = \Gamma_0 + \Gamma_c$. Here we used the fluctuation-dissipation theorem

$$\langle F_{\text{fl}}(t) F_{\text{fl}}(t') \rangle = 2mk_B T_0 \Gamma_0 \delta(t - t') \quad (6)$$

Integrating the PSD provides the variance of q :

$$\langle q^2 \rangle = \frac{k_B T_0}{2m\Omega_0^2} \frac{\Gamma_0}{\Gamma_{\text{tot}}} \quad (7)$$

From the fact that the variance of q is also represented by $q_0^2/2$, we obtain a self-consistent equation for q_0 :

$$q_0^2 = \frac{k_B T_0}{m \Omega_0^2} \frac{\Gamma_0}{\Gamma_{\text{tot}}} \quad (8)$$

By solving this equation, we arrive at the representation for the temperature with electric feedback as shown in eq.(3).

Derivation of the shift in the oscillation frequency induced by a dc electric field

The optical lattice potential is given by

$$U_1(z) = \frac{U_0}{2} \left[1 - \cos\left(\frac{4\pi z}{\lambda}\right) \right] \quad (9)$$

with U_0 the potential depth. The oscillation frequency without a gradient Ω_{z0} is related to U_0 by

$$U_0 = \frac{m \Omega_{z0}^2 \lambda^2}{8\pi^2} \quad (10)$$

The gradient from the DC electric field and the radiation pressure F_0 is

$$U_2(z) = (neV/d_{\text{eff}} + F_0)z \quad (11)$$

The minimum of $U_{\text{tot}}(z) = U_1(z) + U_2(z)$ appears at $z = z_0$ satisfying $dU_{\text{tot}}(z_0)/dz = 0$, which is written as

$$\sin\left(\frac{4\pi z_0}{\lambda}\right) = -\frac{\lambda (neV/d_{\text{eff}} + F_0)}{2\pi U_0} \quad (12)$$

The oscillation frequency around $z = z_0$ can be obtained by calculating the second derivative of $U_{\text{tot}}(z)$:

$$\begin{aligned} \Omega_z^2 &= \frac{1}{m} \frac{d^2 U_{\text{tot}}}{dz^2} \\ &= \frac{8\pi^2 U_0}{m \lambda^2} \cos\left(\frac{4\pi z_0}{\lambda}\right) \end{aligned} \quad (13)$$

Substituting the expressions (10) and (12), we obtain a representation for Ω_z as shown in eq. (4).

[1] M. Lewenstein, A. Sanpera, V. Ahufinger, B. Damski, A. Sen, and U. Sen, *Adv. Phys.* **56**, 243 (2007).
[2] I. Bloch, J. Dalibard, and W. Zwerger, *Rev. Mod. Phys.* **80**, 885 (2008).
[3] R. Blatt and C. F. Roos, *Nat. Phys.* **8**, 277 (2012).
[4] H. Häffner, C. F. Roos, and R. Blatt, *Phys. Rep.* **469**, 155 (2008).
[5] M. Takamoto, F.-L. Hong, R. Higashi, and H. Katori, *Nature* **435**, 321 (2005).

[6] T. Rosenband, D. Hume, P. Schmidt, C.-W. Chou, A. Brusch, L. Lorini, W. Oskay, R. E. Drullinger, T. M. Fortier, J. Stalnaker, et al., *Science* **319**, 1808 (2008).
[7] D. Leibfried, R. Blatt, C. Monroe, and D. Wineland, *Rev. Mod. Phys.* **75**, 281 (2003).
[8] J. Chan, T. M. Alegre, A. H. Safavi-Naeini, J. T. Hill, A. Krause, S. Gröblacher, M. Aspelmeyer, and O. Painter, *Nature* **478**, 89 (2011).
[9] J. Teufel, T. Donner, D. Li, J. Harlow, M. Allman, K. Cicak, A. Sirois, J. D. Whittaker, K. Lehnert, and R. W. Simmonds, *Nature* **475**, 359 (2011).
[10] O. Romero-Isart, A. C. Pflanzer, F. Blaser, R. Kaltenbaek, N. Kiesel, M. Aspelmeyer, and J. I. Cirac, *Phys. Rev. Lett.* **107**, 020405 (2011).
[11] A. Bassi, K. Lochan, S. Satin, T. P. Singh, and H. Ulbricht, *Rev. Mod. Phys.* **85**, 471 (2013).
[12] J. Chaste, A. Eichler, J. Moser, G. Ceballos, R. Rurali, and A. Bachtold, *Nat. Nanotech.* **7**, 301 (2012).
[13] Y. Yang, C. Callegari, X. Feng, K. Ekinci, and M. Roukes, *Nano Lett.* **6**, 583 (2006).
[14] B. C. Stipe, H. J. Mamin, T. D. Stowe, T. W. Kenny, and D. Rugar, *Phys. Rev. Lett.* **87**, 096801 (2001).
[15] J. Moser, J. Güttinger, A. Eichler, M. J. Esplandiu, D. Liu, M. Dykman, and A. Bachtold, *Nat. Nanotech.* **8**, 493 (2013).
[16] G. Ranjit, M. Cunningham, K. Casey, and A. A. Geraci, *Phys. Rev. A* **93**, 053801 (2016).
[17] D. Hempston, J. Vovrosh, M. Toroš, G. Winstone, M. Rashid, and H. Ulbricht, *Appl. Phys. Lett.* **111**, 133111 (2017).
[18] E. Hebestreit, M. Frimmer, R. Reimann, and L. Novotny, *Phys. Rev. Lett.* **121**, 063602 (2018).
[19] P. K. Shukla and B. Eliasson, *Rev. Mod. Phys.* **81**, 25 (2009).
[20] T. Li, S. Kheifets, and M. G. Raizen, *Nat. Phys.* **7**, 527 (2011).
[21] J. Gieseler, B. Deutsch, R. Quidant, and L. Novotny, *Phys. Rev. Lett.* **109**, 103603 (2012).
[22] N. Kiesel, F. Blaser, U. Delić, D. Grass, R. Kaltenbaek, and M. Aspelmeyer, *Proc. Nat. Acad. Sci.* **110**, 14180 (2013).
[23] J. Millen, P. Z. G. Fonseca, T. Mavrogordatos, T. S. Monteiro, and P. F. Barker, *Phys. Rev. Lett.* **114**, 123602 (2015).
[24] J. Vovrosh, M. Rashid, D. Hempston, J. Bateman, M. Paternostro, and H. Ulbricht, *J. Opt. Soc. Am. B* **34**, 1421 (2017).
[25] A. Setter, M. Toroš, J. F. Ralph, and H. Ulbricht, *Phys. Rev. A* **97**, 033822 (2018).
[26] V. Jain, J. Gieseler, C. Moritz, C. Dellago, R. Quidant, and L. Novotny, *Phys. Rev. Lett.* **116**, 243601 (2016).
[27] D. Goldwater and J. Millen, *arXiv preprint arXiv:1802.05928* (2018).
[28] M. Yoneda and K. Aikawa, *J. Phys. B: At. Mol. Opt. Phys.* **50**, 245501 (2017).
[29] M. Yoneda, M. Iwasaki, and K. Aikawa, *Phys. Rev. A* **98**, 053838 (2018).
[30] M. Frimmer, K. Luszcz, S. Ferreira, V. Jain, E. Hebestreit, and L. Novotny, *Phys. Rev. A* **95**, 061801 (2017).
[31] See Supplemental Materials for the derivation of our theoretical models.
[32] In our optical setup, the radiation pressure is finite because the retro-reflected beam has a lower intensity than the incident beam.
[33] E. Hebestreit, R. Reimann, M. Frimmer, and L. Novotny, *Phys. Rev. A* **97**, 043803 (2018).
[34] J. Millen, T. Deesuwan, P. Barker, and J. Anders, *Nat. Nanotech.* **9**, 425 (2014).
[35] E. Hebestreit, M. Frimmer, R. Reimann, C. Dellago, F. Ricci, and L. Novotny, *Rev. Sci. Instr.* **89**, 033111 (2018).